

1 **Decadal changes in bathymetry of the Yangtze River Estuary: human impacts and**
2 **potential saltwater intrusion**

3 **Shuaihu Wu ^{1,2}, Heqin Cheng ^{1,*}, Y.Jun Xu ^{2,*}, Jiufa Li ¹, Shuwei Zheng ¹**

4 1 State Key Lab of Estuarine & Coastal Research, East China Normal University, Shanghai 200062, China;
5 wushuaihuxiaolaoda@163.com

6 2 School of Renewable Natural Resources, Louisiana State University Agricultural Center, 227 Highland Road,
7 Baton Rouge, LA 70803, USA; yjxu@lsu.edu

8 * Correspondence: hqch@sklec.ecnu.edu.cn; Tel.: +86-1376181131; +86-021-62546441(Heqin Cheng)
9 yjxu@lsu.edu; Tel.: +1-225-578-4168; +1-225-578-4227(Y. Jun Xu)

10
11
12
13
14
15
16
17
18
19
20
21
22
23
24
25

26 **Abstract:** This study analyzed bathymetric changes of the 77-km Yangtze River Estuary in
27 China over the past ten years in order to understand the impacts of recent human activities on
28 the estuary of a large alluvial river. Morphological changes were assessed by analyzing
29 digitized bathymetric data of the estuarine channels from 2002 to 2013. Additionally,
30 multi-beam bathymetric measurements made in 2012, 2014 and 2015 were utilized to
31 investigate microtopographic bedforms of the lower reach of the estuary. Our results showed
32 that the middle and upper reaches of the Yangtze River Estuary experienced substantial
33 channel bed erosion in the past 10 years. A sharp decline of sediment supply was found
34 mainly due to the recent human activities in the South Channel and the middle and upper
35 reaches of the North Channel. These included the construction of a 70 km² reservoir along the
36 Yangtze River Estuary, the Qingcaosha Reservoir, for drinking water supply for the City of
37 Shanghai, which has caused progressive bed erosion in the North Channel. The net volume of
38 channel erosion in the Hengsha Passage from 2002 to 2013 was $0.86 \times 10^8 \text{ m}^3$. A large
39 amount of the eroded sediment was trapped downstream, causing overall accretion in the
40 upper reach of the North Passage. The middle and upper reaches of the South Passage also
41 experienced intense erosion ($0.45 \times 10^8 \text{ m}^3$) in the past ten years, while high accretion
42 occurred in the lower reach because of the Deepening Waterway Project. The channel
43 dredging left a large range of dredging marks and hollows in the North Passage. The
44 increasing saltwater intrusion found in the Yangtze River Estuary may have been a
45 consequence of either dredging or erosion, or both combined.

46 **Keywords:** estuarine morphology; bathymetric dynamics; saltwater intrusion; estuarine
47 bedforms; multi-beam profiling; Yangtze River Estuary

48

49

50 **1. Introduction**

51 Many estuaries in the world have been interrupted by human activities, such as the
52 damming of the river, building of reservoir and dredging for waterway (Blott et al., 2006;
53 Benedet and List., 2008; Talke et al., 2009; Day et al., 1989). Remarkable consequences of
54 these human activities in estuaries include morphological changes of the channel beds and
55 saltwater intrusion; they have therefore been the foci of several scientific enquiries (Thomas
56 et al., 2002; Nichols and Howard-Strobel., 1991; Gong et al., 2012).

57 Several studies have indicated that human activities could have pronounced effects on
58 estuarine hydrodynamics and morphology. For instance, in the Ems Estuary in Germany, the
59 estuarine dynamics and the erosion and sedimentation process were affected, pushing the
60 position of the turbidity maximum zone upstream because of channel dredging (De Jonge et
61 al., 2014). Due to the construction of the Aswan Dam, annual erosion rate for the area around
62 Rosetta Promontory was reported to be $10 \times 10^6 \text{ m}^3$ in the Nile delta (Inman and Jenkins.,
63 1984). Lane (2004) reported that the volume of the Mersey Estuary in UK decreased by 0.1%
64 in the past 150 years because of channels dredging and construction of retaining walls.

65 Seawater intrusion has been found to have intensified across the world in the recent
66 decades due to human activities (Savenije., 2005; Barlow and Reichard., 2010). For instance,
67 Yuan and Zhu (2015) found that dredging in the Pearl River estuary in China has strongly
68 affected saltwater instruction. Omar et al. (2016) reported that over-pumpage of aquifers in
69 the Mediterranean region has led to intensified seawater intrusion. However, few studies have
70 investigated human effects on channel morphology of large alluvial river estuaries, such as
71 the Yangtze River Estuary in China.

72 The Yangtze River Estuary is a continental-scale alluvial estuary, which has gone
73 through many physical alterations for flood control, navigation, port construction, and urban
74 development of the City of Shanghai, the most vibrant and largest economy in China.

75 Shanghai is located near the Yangtze River Estuary and the Yangtze River is the major source
76 of freshwater supply for the city. There are four large drinking water reservoirs within the
77 estuary area that provide freshwater for about 50 million people living on the Yangtze River
78 Delta. Like other tidal-controlled estuaries, the Yangtze River Estuary has been found to be
79 affected by saltwater intrusion in recent years (Cheng and Zhu., 2013). This has raised serious
80 concerns over freshwater supply (Wu and Zhu., 2010; Li et al., 2012a; Mao et al., 2001) and
81 future economic development in the region (Chen et al., 2016).

82 Human interventions in the Yangtze River basin, e.g., the construction of the Three
83 Gorge Dam (TGD) in the middle reach of the Yangtze River, have changed flow conditions in
84 the river's lower reach and estuary (Zhang et al., 2009). In the recent decade, two large
85 engineering projects - the Yangtze estuarine Deepening Waterway project and the Qingcaosha
86 Reservoir project - may have particularly affected the morphology of the Yangtze River
87 Estuary. Several studies (Jiang et al., 2012; Li et al., 2008; Liu et al., 2005; Dai et al., 2013)
88 reported a morphological change of several sand bars of the Yangtze River mouth. However,
89 very few studies have investigated changes across the entire lower estuary reach. Little is
90 known for other parts of the large Yangtze River Estuary impacted by human interventions. In
91 general, there is a knowledge gap as to how the Yangtze River Estuary channel has changed
92 in the recent decade and whether these changes have played a role in saltwater intrusion. A
93 study focusing on such a nature-human coupled complex system has important significance
94 for improving our knowledge of human effects not only on the Yangtze River Estuary but
95 also on other alluvial river estuaries in the world. Such knowledge can be crucial for
96 developing effective management plans for coastal protection against sea level rise, erosion
97 and land loss.

98 This study aimed to assess the recent morphological changes of the channel beds using
99 bathymetric survey charts, high-resolution multi-beam data, river discharge and sediment load

100 data. The primary goal was to document bathymetry change in the Yangtze River Estuary in
101 order to understand the relationship between human activities and the channel morphology, as
102 well as the potential risk of saltwater intrusion. Results gained from this work can be useful
103 for river channel morphology research, river water management and coastal protection. It can
104 also serve as an example for the remediation and development of other estuaries under similar
105 natural and anthropogenic influences.

106 **2. Methods**

107 *2.1. Study area*

108 Draining a land mass of approximately 1.8 million km², the Yangtze River (Fig. 1) is the
109 world's fourth largest river in terms of sediment load (Yang et al., 2005). There is a tidal
110 influence in the Yangtze River extending 650 km upstream. The last 120 km section of the
111 estuary below Xuliujing shows a "three-consecutive bifurcations with four outlets. It is first
112 divided into the South and North Branches by the Chongming Island (Fig. 1). The South
113 Branch is then divided into the South and North Channels by the Changxing Island and the
114 Hengsha Island. The South Channel is again divided by the Jiudian Shoal into the South and
115 North Passages. The mouth bar section is geographically located between 121°45'-122°30' E
116 and 30°45'-31°45' N (Fig 2A). The turbidity maximum zone exists in the river mouth-bar area
117 all year round, with high solid concentrations due to the interaction of freshwater and tidal
118 flows (Chao et al., 2015; Li and Wu., 2011).

119 Long-term discharge at Datong Hydrological Gauging Station, located about 600 km
120 upstream from the river mouth, averaged 29 300 m³/s (Cheng et al., 2004). The river flow
121 fluctuates seasonally, generally low in January or February (dry season) and high during July
122 or August (wet season) (Pu et al., 2015). The annual mean suspended sediment load from the
123 Yangtze River from 1956 to 2009 was 388.6 million tons (Jiang et al., 2012). It has been

124 estimated that 40% of the annual sediment load is deposited in the Yangtze River Estuary
125 (Zhu et al., 2015). The sediment deposit in the Yangtze River Estuary is mainly composed of
126 fine sand, silt and clay (Liu et al., 2010).

127 The Yangtze River Estuary is characterized as a mesotidal estuary in terms of tidal range
128 (Wu et al., 2009). Tides are regular semi-diurnal out of the mouth, and non-regular
129 semi-diurnal inside. The long-term mean tidal range at Zhongjun Station nearby the mouth is
130 about 2.67 m, with a tidal velocity amplitude of approximately 1 m/s (Yang et al., 2015a).

131 *2.2. Bathymetric data collection*

132 Digitized bathymetry-derived Digital Elevation Model (DEM) has become a useful tool
133 to study morphological changes of estuaries (Thomas et al., 2002; Lane., 2004; Blott et al.,
134 2006; Jaffe et al., 2007). In order to investigate the morphological changes in the Yangtze
135 River Estuary, the bathymetric surveys have been carried out by the Changjiang Estuary
136 Waterway Administration Bureau (CJWAB), Ministry of Transportation. The digital survey
137 charts of 2002 and 2007 were used in this study. The bathymetric survey charts for 2010 and
138 2013 in the South and North Channels, and the South and North Passages, provided by
139 Shanghai Estuarine & Coastal Science Research Center, were also used in this study. The
140 marine charts of 2012 in the North Channel and 2013 in the Hengsha Passage, provided by
141 Maritime Safety Administration of the People's Republic of China (PRC), were also used to
142 investigate the morphological changes. The marine charts (1:15000 scales) were digitalized
143 and used in our GIS analysis (Table 1).

144 The long-term discharge and sediment load monitored at the Datong station located at the
145 landward limit of the tidal river between 2002 and 2013 published in the Yangtze River
146 Sediment Bulletin, were used to interpret the cause of the morphological changes in the study
147 area.

148 *2.3. Riverbed multibeam measurements*

149 The bedforms of the South and North Channels, the South and North Passages, and the
150 Hengsha Passage in the Yangtze River Estuary were observed by using a Reson Seabat 7125
151 MBES (Teledyne Technologies Inc, Thousand Oaks, CA, USA) during December 2012,
152 February 2014 and February 2015 (Fig. 2A). The seabat 7125 was operated at the working
153 frequency of 400 kHz, and the transducer was mounted on the left side of the surveying ship
154 by cables and a custom-made shelf. The highest depth resolution is 6 mm. The boat speed was
155 controlled to be as steady as possible at 2.5 m/s. Weather condition was good during the
156 survey period.

157 *2.4 Data analysis*

158 The bathymetric data and charts were digitized and analyzed through creating DEM with
159 ArcGIS software (Fig. 3). First, all charts were georeferenced using ten fixed benchmarks,
160 with known National Grid coordinates. The depth values were transformed into the Beijing
161 1954 coordinates in Gauss-Kruger Zone 21 N. The Theoretical Lowest Tide Level (which is
162 based on 13 tidal components) was used as the datum for elevations and depths. Subsequently,
163 the Kriging interpolation technique, a widely used method in morphological change analysis
164 of estuaries (Zhao et al., 2015; Van der Wal et al., 2002; Van der Wal and Pye., 2003), was
165 utilized to interpolate each data set to a grid with 200×200 m resolution on the ArcGIS 9.3
166 platform.

167 By subtracting the depth of one year from that of another, the changes of bathymetry and
168 14 cross-sectional areas (Fig. 2B) were determined. To quantify erosion or deposition rates,
169 the volume changes were calculated between 2002 and 2013, which provided basis for
170 sediment mass estimation. The generally errors associated with bathymetric change and
171 sediment volume based on bathymetry and the Kriging interpolation technique were estimated
172 to be less than 10% (Jiang et al., 2012).

173 The final multi-beam data were processed by draft correction, sound speed correction,
174 and correction for roll, pitch, and yaw. Abnormal beam was removed in the editing module by
175 using PDS 2000 software (Teledyne RESON, Slangerup Denmark). Tidal data at Wusong
176 station were used for tidal correction. The vertical datum of the Wusong tide station level is
177 202 cm lower than mean sea level. By using the Trimble real-time differential global
178 positioning system (DGPS), the accuracy was at the decimeter level.

179 **3. Results**

180 *3.1. Bathymetric changes*

181 For the 77-km North Channel, the bed erosion, accretion and net sediment change in
182 volume before the construction of the Qingcaosha Reservoir project (2002~2007) were 5.49
183 $\times 10^8 \text{ m}^3$, $4.51 \times 10^8 \text{ m}^3$ and $0.98 \times 10^8 \text{ m}^3$, respectively (Fig. 4A). After the project was
184 constructed in 2007, the bed erosion rate nearly doubled ($9.84 \times 10^8 \text{ m}^3$), while the accretion
185 rate remained almost unchanged ($4.29 \times 10^8 \text{ m}^3$), resulting in 5 times higher net volume loss
186 ($5.56 \times 10^8 \text{ m}^3$) (Fig. 4B). Overall, during 2002-2013, net volume loss and average annual net
187 volume loss reached $6.54 \times 10^8 \text{ m}^3$ and $0.65 \times 10^8 \text{ m}^3 \text{ yr}^{-1}$, respectively (Fig. 4C).

188 For the 35-km South Channel, during the period 2002-2013, the bed erosion, accretion,
189 net volume loss and average annual net volume loss reached $2.97 \times 10^8 \text{ m}^3$, $1.61 \times 10^8 \text{ m}^3$,
190 $1.36 \times 10^8 \text{ m}^3$ and $0.12 \times 10^8 \text{ m}^3 \text{ yr}^{-1}$, respectively (Fig. 5A).

191 For the 9-km Hengsha Passage, the bed erosion, accretion and net sediment loss in
192 volume between 2002 and 2007 were $0.66 \times 10^8 \text{ m}^3$, $0.45 \times 10^8 \text{ m}^3$ and $0.21 \times 10^8 \text{ m}^3$,
193 respectively (Fig. 6A). During 2007-2013, the bed erosion rate was slightly higher (0.84×10^8
194 m^3), while the accretion rate reduced by nearly two thirds ($0.19 \times 10^8 \text{ m}^3$), resulting in 3 times
195 higher net volume loss ($0.65 \times 10^8 \text{ m}^3$) (Fig. 6B). Overall, from 2002 to 2013, net volume loss

196 and average annual net volume loss reached $0.86 \times 10^8 \text{ m}^3$ and $0.08 \times 10^8 \text{ m}^3 \text{ yr}^{-1}$, respectively
197 (Fig. 6C).

198 For the 60-km South Passage, during the period of Deepening Waterway Project in the
199 North Passage (NP) of the Yangtze River Estuary (2002–2010), the bed erosion, accretion and
200 net sediment loss in volume were estimated to be $8.31 \times 10^8 \text{ m}^3$, $3.63 \times 10^8 \text{ m}^3$ and 4.68×10^8
201 m^3 , respectively (Fig. 6D). After the completion of the Deepening Waterway Project
202 (2010-2013), the bed erosion was greatly reduced to $3.02 \times 10^8 \text{ m}^3$, while the accretion rate
203 reduced slightly ($2.72 \times 10^8 \text{ m}^3$), resulting in 15 times lower net volume loss ($0.3 \times 10^8 \text{ m}^3$)
204 (Fig. 6E). Overall, during the period from 2002 to 2013, net volume loss and average annual
205 net volume loss reached $4.98 \times 10^8 \text{ m}^3$ and $0.45 \times 10^8 \text{ m}^3 \text{ yr}^{-1}$, respectively (Fig. 6F).

206 During 2010-2013, the depth of the waterway was increased in the North Passage (Fig. 5B)
207 due to the dredging project. Therefore, no attempt was made to calculate bed erosion and
208 accretion for the North Passage.

209 *3.2. Changes in cross-sectional areas*

210 Cross-section NC1 (Fig. 7) in the middle and upper reaches of the North Channel clearly
211 showed that the northern side experienced about 5 m channel erosion during 2002-2007,
212 while about 5.5 m channel accretion occurred in the central part. The deep trough moved
213 northward in 2007, and the maximum water depth changed from 15 m to 17 m. Between 2007
214 and 2013 about 3 m and 2 m channel erosion occurred in the northern side and central part,
215 respectively. Cross-section NC2 (Fig. 7) in the upper reach of the mouth bar area of the North
216 Channel showed that the northern and southern sides were scoured about 3 m, respectively,
217 while about 4 m accretion occurred in the central part between 2002 and 2007. During
218 2007-2013, the southern side experienced about 3 m erosion, while about 0.5 m and 1 m
219 accretion occurred in the northern side and central part, respectively. Cross-section NC3 (Fig.
220 7) in the middle and lower reaches of the mouth bar area of the North Channel showed that

221 the northern side and central part experienced about 0.5 m and 1 m erosion, respectively,
222 while about 2 m accretion occurred in the southern side from 2002 to 2007. During
223 2007-2013, the channel in the northern side and central part were scoured about 1 m and 1.5
224 m, respectively, while strong accretion occurred in the central part (i.e., about 2 m). During
225 2002-2013, the area of the cross-section NC1 increased 12.4%, while the cross-sections NC2
226 and NC3 decreased 0.2% and 0.3%, respectively (Table 2).

227 During the period from 2002 to 2013, cross-section SC1 (Fig. 7) in the upper reach of the
228 South Channel showed that the northern side and central part experienced about 3 m and 2 m
229 channel erosion, respectively, while less marked morphological change occurred in the
230 southern side. Cross-section SC2 (Fig. 7) in the middle reach showed about 5 m and 2 m
231 erosion in the northern side and central part, respectively, while slight accretion of 1m
232 occurred in the southern side. Cross-section SC3 (Fig. 7) in the lower reach showed a similar
233 pattern of morphological changes to cross-section SC2, which included strong erosion in the
234 northern side and central part, as well as slight accretion in the southern side. During
235 2002-2013, the area of the cross-sections SC1, SC2 and SC3 increased 9.7%, 12.3% and
236 11.8%, respectively (Table 2).

237 Cross-section HP1 (Fig. 8) in the north entrance of the Hengsha Passage was scoured
238 entirely between 2002 and 2007, and the main channel shifted toward the Changxing Island.
239 During 2007-2013, the channel in the eastern bank and central part were scoured about 9 m
240 and 23 m, respectively, while a sudden accretion of about 0.2 m occurred in the western bank.
241 The main channel was close to the Hengsha Island with the maximum water depth of 30 m.
242 Cross-section HP2 (Fig. 8) in the middle reach showed that about 7 m accretion and about 3
243 m erosion occurred in the central part and the western bank, respectively, while the eastern
244 bank showed less marked morphological change during 2002-2007. Between 2007 and 2013
245 the eastern bank, central part and western bank were scoured about 12 m, 6 m and 2.5 m,

246 respectively. Cross-section HP3 (Fig. 8) in the south entrance clearly showed about 2 m and 1
247 m erosion in the eastern bank and western bank, respectively, while strong accretion of about
248 3 m occurred in the central part during 2002-2007. From 2007 to 2013, the eastern bank and
249 central part were scoured about 6 m and 4 m, respectively, while about 4.5 m accretion
250 occurred in the western bank. During the period from 2002 to 2013, the area of the
251 cross-sections HP1, HP2 and HP3 increased 137.2%, 46.4% and 50%, respectively (Table 3).

252 Cross-section SP1 (Fig. 8) in the upstream opening of the South Passage was heavily
253 scoured between 2002 and 2010. The deep trough moved southward in 2010, and the
254 maximum water depth increased from 10.5 to 12 m. During 2010-2013, the channel in the
255 central part and southern side were scoured about 2 m and 1.5 m, respectively, while the
256 northern side experienced about 1m accretion. Cross-section SP2 (Fig. 8) in the upper reach
257 of the South Passage showed continual erosion in the northern side and central part between
258 2002 and 2013, while less marked morphological change occurred in the southern side.
259 Cross-section SP3 (Fig. 8) in the middle reach showed that the northern side and central part
260 experienced about 1 m and 2 m erosion, respectively, while about 3 m accretion occurred in
261 the southern side during 2002-2010. From 2010 to 2013, the southern side experienced
262 continual accretion of approximately 2.5 m, while the northern side and central part showed
263 less marked morphological change. Cross-section SP4 (Fig. 8) in the lower reach experienced
264 distinct accretion entirely between 2002 and 2010. During 2010-2013, about 1 m erosion and
265 0.5 m accretion occurred in the northern side and southern side, respectively, while the central
266 part showed less marked morphological change. During the period from 2002 to 2013,
267 cross-section SP5 (Fig. 8) on the outer estuary showed that the northern side and central part
268 were scoured about 0.5 m and 1 m, respectively, while less marked morphological change
269 occurred in the southern side. During 2002-2013, the area of the cross-sections SP1, SP2, SP3

270 and SP5 increased 18.1%, 18.7%, 12.6% and 8.6%, respectively, while the area of the
271 cross-section SP4 decreased 7.3% (Table 3).

272 *3.3. Changes in the longitudinal profiles*

273 The longitudinal profile of the North Channel has two peaks (shallow area), and the
274 minimum water depth was approximately 5 m in 2002. During 2002-2013, the middle and
275 upper reaches experienced strong erosion, while distinct siltation occurred in the mouth bar
276 area (Figs. 2B and 9).

277 The longitudinal profile of the South Channel showed continual channel erosion during
278 2002-2013 (Figs. 2B and 9). The middle and upper reaches experienced strong erosion and
279 the local depth reached a maximum of 19 m. The water depth increased from 10 m to 12.5 m
280 in the lower reach.

281 The longitudinal profile of the Hengsha Passage showed that the north entrance
282 experienced strong erosion between 2002 and 2007, while strong accretion occurred in the
283 middle reach and south entrance (Figs. 2B and 9). During 2007-2013, the continual channel
284 erosion occurred in the entire Hengsha Passage, especially the north entrance experienced
285 extremely strong erosion and the local depth reached a maximum of 27 m.

286 The longitudinal profile of the South Passage has two peaks (shallow area), and the
287 minimum water depth was approximately 5.5 m in 2002 (Figs. 2B and 9). During 2002-2013,
288 intense channel erosion occurred in the middle and upper reaches, while gradual accretion
289 occurred in the lower reach.

290 **4. Discussion**

291 *4.1. Variations in discharge and sediment input into the Yangtze River Estuary*

292 Under the influence of the strong human interventions within the Yangtze River basin
293 such as dam construction, water and soil conservation, and river sand mining in recent years,

294 the riverine conditions has changed significantly, especially after the construction of the
295 Three Gorge Dam (TGD) which began to impound water in June 2003 (Zhang., 2009).
296 Although the discharge at the Datong station did not show noticeable change since 2003,
297 sediment supply in the past decade showed a declining trend (Fig. 10). This may has inducing
298 an increased sediment-carrying capacity of flow, which may have contributed to bed erosion
299 of the South Channel and the middle and upper reaches of the North Channel (Figs. 4 and 5A).
300 However, the decrease in the sediment supply to the Yangtze River Estuary only marginally
301 affected morphological changes in the South and North Passages (Jiang et al., 2012; He et al.,
302 2013).

303 *4.2. Influence of local engineering projects*

304 The morphology and topography of the North Channel have been changed significantly
305 due to human interventions, especially the construction of the Qingcaosha Reservoir project
306 (Li et al., 2012b). Before the project (2002-2007), there was erosion in the middle and upper
307 reaches, while accretion occurred in the upper reach of the mouth bar area. After execution of
308 the project started (2007-2012), a large part of the upper North Channel was confined by
309 levees, causing narrowing of the channel from 7.1 km to 4.3 km. This has caused large
310 channel incising and bed scouring. The eroded sediment was transported seaward from the
311 middle and upper reaches, resulting in substantial accretion in the upper reach of the mouth
312 bar area. As the scouring trend continues (Liu et al., 2011a), the upper reach of the mouth bar
313 area also experienced erosion. Hence, the eroded sediment was transported seaward from the
314 upper reach of the mouth bar area, causing strong accretion in the middle and lower reaches
315 of the mouth bar area.

316 The Hengsha Passage is a unique passage oriented in the N-S direction in the Yangtze
317 River Estuary with the North Channel in its north and the North Passage in its South. The

318 development of the channel was believed to be caused by the phase difference in tidal due to
319 estuarine bifurcation (Kuang et al., 2014). This may be also related to the sediment and water
320 exchange between the North Channel and the North Passage (Cheng et al., 2010). The
321 construction of the Qingcaosha Reservoir project and Changxing Submerged Dike project
322 may have indirectly affected the morphology of the Hengsha Passage (Kuang et al., 2014).
323 The Changxing Submerged Dike project is a part of the Deepening Waterway Project, which
324 is located on the sand spit in the southeast of the Changxing Island with a length of 1 840 m.
325 Before the projects (2002-2007), there was erosion in the north entrance, while accretion
326 occurred in the middle reach and south entrance. After execution of the projects (2007-2013),
327 analysis showed that the middle and upper reaches of the North Channel experienced strong
328 erosion, while the north entrance, middle reach and south entrance in the Hengsha Passage
329 also experienced constant erosion during the same period. A large amount of the eroded
330 sediment from the south entrance of the Hengsha Passage was trapped, resulting in substantial
331 accretion in the upper reach of the North Passage (Figs. 5). Consequently, a large range of
332 scour marks is clearly visible in the bed of the Hengsha Passage (Fig. 11 A).

333 The ebb flow diversion ratios in the North Passage and the South Passage (the percentage
334 of ebb tidal volume of the North Passage and the South Passage in the total ebb tidal volume)
335 were reported to be about 60% and 40%, respectively, before 1998 when construction of the
336 Deepening Waterway Project was started (Kuang et al., 2014). During the first construction
337 stage of the Project (August 1998–May 2001), two training walls and ten groins were
338 constructed in the North Passage, which led to a significant change in the ebb flow diversion
339 ratio in both the North Passage and the South Passage (Jiang et al., 2012). From the second to
340 the third construction stage (2002-2010), the ebb flow diversion ratio of the South Passage
341 increased significantly, for example, the minimum ebb flow diversion ratio increased from
342 60% to 70% during the flood season of 2010 (Dai et al., 2015). These findings indicate that

343 the stronger ebb flow may have been the cause for the estuarine bed erosion in the upper
344 reach and the consequent accretion in the lower reach.

345 The North Passage has been affected by the Deepening Waterway Project carried out in
346 the Yangtze River Estuary between 1998 and 2010 (Song et al., 2013). The main channel has
347 been continually dredged since 1998 from the average water depth of less than 7 m to the
348 present 12.5 m using trailing-suction hopper dredgers (Chen et al., 2015). The water depth of
349 the waterway reached 12.5 m by 2010, and the back siltation increased obviously in the
350 waterway (Jiang et al., 2012). The quantity of back siltation was 80.9 million m³ between
351 February 2010 and August 2011, and the back siltation mainly concentrated in the middle
352 reach of the North Passage (Ge et al., 2013; Dai et al., 2013; Song and Wang., 2013; Liu et al.,
353 2011b). Therefore, in order to maintain a deep waterway, dredging must be carried out on a
354 continual basis; indeed the annual dredged volume has increased in recent years to more than
355 $6 \times 10^7 \text{m}^3$ (Kuang et al., 2014). A large number of dredging marks and hollows have therefore
356 become apparent in recent years in the North Passage (Figs. 11B and 11 C).

357 *4.3 Saltwater intrusion*

358 Salinity is a key parameter describing aquatic systems in an estuarine environment
359 (Huang and Foo., 2002). Understanding salinity variation in estuaries under different forcing
360 conditions, e.g. extreme drought, climate change or human interventions, can be crucial for
361 helping manage estuarine water resources (Brockway et al., 2006). Salinity in the Yangtze
362 River Estuary is affected by river discharge and oceanic saltwater (An et al., 2009). River
363 discharge freshen the estuary, whereas tide transports salt into the estuary and increases
364 salinity. It is understood that when the salinity level in the Yangtze River Estuary is over 100
365 mg/l, saltwater intrusion is assumed to occur (Chinese living drinking water and water source
366 standard (CJ302093)).

367 However, saltwater intrusion in the Yangtze River Estuary may be affected by
368 bathymetry change caused by human interventions in the recent years. It is well known that
369 increased depth can lead to increased saltwater intrusion. It is more complicated why depth
370 increase would lead to saltwater intrusion. Deeper depth would lead to stronger vertical
371 circulation resulting in more saltwater transported upstream at the bottom.

372 Saltwater transport plays an important role in estuaries and can have impacts on
373 ecological and biogeochemical conditions (Zhou et al., 2008). The residual transports of
374 saltwater in the South Channel are generally seaward and are affected by runoff (Ge et al,
375 2013). With river flow discharge decreasing, saltwater migrates toward the landward and
376 increases mean salinity (Wu et al., 2006). While our study indicated that the South Channel
377 experienced intense erosion in the recent years. Consequently, the water depth has increased,
378 which will aggravate the saltwater intrusion.

379 The North Channel is the major outlet of fresh water in the Yangtze River Estuary and
380 residual transport flows seaward (Cheng and Zhu., 2013), Cheng and Zhu (2015) reported that
381 the North Channel has more pronounced salinity increase than the other channels. This may
382 have been a result from the strong erosion that we found in this study in the middle and upper
383 reaches of the North Channel. The landward saltwater transport is strengthened in the North
384 Channel and may further affect the upper reach (Cheng and Zhu., 2015). This can threaten the
385 security of freshwater resources and the ecosystem in the affected area. The Qingcaosha
386 Reservoir provides an average of 7.19 million m³ freshwater per day, more than half of the
387 daily water supply amount to Shanghai (Yang et al., 2015b). When salinity exceeds 0.45 psu
388 (chlorinity of 250 mg/l), it is considered undrinkable (Dai et al., 2011).

389 Due to the lower freshwater inflow when compared with the North Channel, salinities in
390 the South and North Passages are relatively higher. Residual transport in the upper North
391 Passage is directed seaward, whereas landward transport occurs in the South Passage and the

392 lower North Passage (Cheng and Zhu., 2013). This landward residual transport in the South
393 Passage is mainly caused by tide and topography, and landward transport in the lower North
394 Passage is controlled by tides (Wu and Zhu., 2010). Intense erosion in recent years
395 experienced in the middle and upper reaches of the South Passage, increased water depth may
396 have aggravated saltwater intrusion in the South Passage.

397 Increased depth of the waterway due to dredging in the North passage, may have
398 contributed to increased saltwater intrusion, especially during the flood tide when the
399 high-salinity seawater moves onshore into the North Passage (Ge et al., 2013). Saltwater
400 intrusion may have also played an important role in the siltation of the shipping channel as
401 flocculation occurs in a salinity range of 5-10 psu found in the middle region of the waterway
402 (Ge et al., 2013). Consequently, it is possible that saltwater intrusion has intensified siltation
403 because of the freshwater-saltwater mixing, pushing the turbidity maximum zone inland.

404 **5. Conclusions**

405 This study analyzed the bathymetric changes of the Yangtze River Estuary from 2002 to
406 2013. The results showed that the middle and upper reaches of the estuary experienced strong
407 erosion caused by recent human activities. A large amount of the eroded sediment appeared to
408 be trapped downstream, causing overall channel bed accretion in the lower river mouth reach
409 of the estuary. The navigable depth was deepened in the North Channel because of the
410 construction of a large drinking water reservoir. The South Passage became the chief conduit
411 for seaward transport of sediment because of a channel deepening project. In order to
412 maintain the minimal depth of 12.5 m for the shipping channel, daily dredging amount had to
413 be increased, resulting in more costs in manpower and financial resources. Saltwater intrusion
414 has increased in the South and North Channels, and South and North Passages, likely due to
415 the bathymetry changes caused by human interventions in recent years. These results suggest

416 that human activities have direct effects not only on channel morphology but also on the
417 salinity in the Yangtze River Estuary.

418 **Acknowledgments:** This study was financially supported by the Natural Science Foundation
419 of China (Grant Number: 41476075). During preparation of this manuscript, Shuaihu Wu was
420 supported by an award of the China Scholarship Council (File No.201506140113) and Y. Jun
421 Xu received partial support from a grant of the U.S. National Science Foundation (award
422 number: 1212112) and a U.S. Department of Agriculture Hatch Fund project (project number:
423 LAB94230). We are also grateful for three anonymous reviewers and Editor Steve Mitchell
424 for their helpful comments and suggestions.

425

426 **References**

427 An, Q., Wu, Y.Q., Taylor, S., Zhao, B., 2009. Influence of the Three Gorges Project on
428 saltwater intrusion in the Yangtze River Estuary. *Environ Geol* 56, 1679-1686.

429 Barlow, P.M., Reichard, E.G., 2010. Saltwater intrusion in coastal regions of North America.
430 *Hydrogeol. J* 18, 247–260.

431 Blott, S.J., Pye, K., van der Wal, D., Neal, A., 2006. Long-term morphological change and its
432 causes in the Mersey Estuary, NW England. *Geomorphology* 81, 185-206.

433 Brockway, R., Bowers, D., Hogue, A., Dove, V., Vassele, V., 2006. A note on salt intrusion
434 in funnel-shaped estuarine: Application to the Incomati Estuary, Mozambique. *Estuarine,
435 Coastal and Shelf Science* 66, 1-5.

436 Benedet, L., List, J.H., 2008. Evaluation of the physical process controlling beach changes
437 adjacent to nearshore dredge pits. *Coastal Engineering* 55, 1224-1236.

438 Cheng, H.Q., Kostaschuk, R., Shi, Z., 2004. Tidal Currents, Bed Sediments, and Bedforms at
439 the South Branch and the South Channel of the Changjiang (Yangtze) Estuary, China:
440 Implications for the Ripple-dune Transition. *Estuaries* 27, 861-866.

441 Chao, M., Shi, Y.R., Quan, W.M., Shen, X.Q., 2015. Distribution of Macrocrustaceans in
442 Relation to Abiotic and Biotic Variables across the Yangtze River Estuary, China. *Journal of
443 Coastal Research* 31, 946-956.

444 Cheng, H.F., Liu, J., Zhao, D.Z., 2010. Analysis of river bed evolution and prediction of its
445 trend for Hengsha Passage. *Journal of Waterway and Harbor* 31, 365-369 (in Chinese).

446 Cheng, Q., Zhu, J.R., 2013. Influence of seasonal runoff regulation by the Three Gorges
447 Reservoir on saltwater intrusion in the Changjiang River Estuary. *Continental Shelf Research*
448 71, 16-26.

449 Cheng, Q., Zhu, J.R., 2015. Assessing the influence of Sea Level Rise on Salt Transport
450 Processes and Estuarine Circulation in the Changjiang River Estuary. *Journal of Coastal*
451 *Research* 31, 661-670.

452 Chen, D., Dai, Z.J., Xu, R., Li, D.J., Mei, X.F., 2015. Impacts of anthropogenic activities on
453 the Changjiang (Yangtze) estuarine ecosystem (1998-2012). *Acta Oceanol. Sin* 34, 86-93.

454 Chen, W., Chen, K., Kuang, C.P., Zhu, D.Z., He, L.L., Mao, X.D., Liang, H.D., Song, H.L.,
455 2016. Influence of sea level rise on saline water intrusion in the Yangtze River Estuary, China.
456 *Applied Ocean Research* 54, 12-25.

457 Day, J.W., Hall, C.A.S., Kemp, W.M., Yanez-Arancibia, A., 1989. *Estuarine Ecology*. John
458 Wiley & Sons, Inc., New York, NY, USA.

459 De Jonege, V.N., Schuttelaars, H.M., van Beusekomc, J.E.E., Talke, S.A., de Swart, H.E.,
460 2014. The influence of channel deepening on estuarine turbidity levels and dynamics, as
461 exemplified by the Ems estuary. *Estuarine, Coastal and Shelf Science* 139, 46-59.

462 Dai, Z.J., Chu, A., Stive, M., Zhang, X.L., 2011. Unusual Salinity Conditions in the Yangtze
463 Estuary in 2006: Impacts of an Extreme Drought or of the Three Gorges Dam? *AMBIO* 40,
464 496-505.

465 Dai, Z.J., Liu, J.T., Fu, G., Xie, H.L., 2013. A thirteen-year record of bathymetric changes in
466 the North Passage, Changjiang (Yangtze) estuary. *Geomorphology* 187, 101-107.

467 Dai, Z.J., Liu, J.T., Wei, W., 2015. Morphological evolution of the South Passage in the
468 Changjiang (Yangtze River) estuary, China. *Quaternary International* 380-381, 314-326.

469 Gong, W.P., Wang, Y.P., Jia, J.J., 2012. The effect of interacting downstream branches on
470 saltwater intrusion in the Modaomen Estuary, China. *Journal of Asian Earth Sciences* 45,
471 223-238.

472 Ge, J.Z., Ding, P.X., Chen, C.S., Hu, S., Fu, G., Wu, L.Y., 2013. An integrated East China
473 Sea-Changjiang Estuary model system with aim at resolving multi-scale
474 regional-shelf-estuarine dynamics. *Ocean Dynamics* 63, 881-900.

475 Huang, W.R., Foo, S., 2002. Neural network modeling of salinity variation in Apalachicola
476 River. *Water Research* 36, 356-362.

477 He, Y.F., Cheng, H.Q., Chen, J.Y., 2013. Morphological Evolution of Mouth Bars of the
478 Yangtze Estuarine Waterways. *Journal of Geographical Sciences* 23, 219-230.

479 Inman, D.L., Jenkins, S.A., 1984. The Nile littoral cell and man's impact on the coastal zone
480 of the South East Mediterranean. In: 19 th Coastal Engineering Conference. Proceedings
481 American Society of Civil Engineers, Houston, Texas 1600-1617.

482 Jaffe, B.E., Smith, R.E., Foxgrover, A.C., 2007. Anthropogenic influence on sedimentation
483 and intertidal mudflat change in San Pablo Bay, California: 1856-1983. *Estuarine, Coastal
484 and Shelf Science* 73, 175-187.

485 Jiang, C.J., Li, J.F., de Swart, H.E., 2012. Effects of navigational works on morphological
486 changes in the bar area of the Yangtze River Estuary. *Geomorphology* 139, 205-219.

487 Kuang, C.P., Chen, W., Gu, J., He, L.L., 2014. Comprehensive ananlysis on the sediment
488 silation in the upper reach of the deep-water navigation channel in the Yangtze Estuary.
489 *Journal of Hydrodynamics* 26, 299-308.

490 Lane, A., 2004. Bathymetric evolution of the Mersey Estuary, UK, 106-1997: causes and
491 effects. *Estuarine, Coastal and Shelf Science* 59, 249-263.

492 Li, X., Wu, D.A., 2011. Study on the Yangtze River estuarine turbidity maximum. *Applied
493 Mechanics and Materials*, 90-93, 2774-2747.

494 Li, W.H., Cheng, H.Q., Li, J.F., Dong, P., 2008. Temporal and spatial changes of dunes in the
495 Changjiang (Yangtze) estuary, China. *Estuarine, Coastal and Shelf Sciences* 77, 169-174.

496 Li, L., Zhu, J.R., Wu, H., 2012a. Impacts of wind stress on saltwater intrusion in the Yangtze
497 Estuary. *Science China Earth Sciences* 55, 1178-1192 (in Chinese).

498 Li, B.C., Wang, J., Tang, M.J., 2012b. Analysis on recent evolution of Beigang branch of
499 Yangtze River Estuary and its regulation countermeasures. *Yangtze River* 43, 12-16 (in
500 Chinese).

501 Liu, J., Chen, J.Y., Le, J.H., Huang, R.Y., 2005. Effect of the implementation of the
502 first_stage project of the deepwater channel regulation in the Yangtze River Estuary on the
503 erosion and deposition in the South Passage. *Journal of Sediment Research* 5, 40-44 (in
504 Chinese).

505 Liu, H., He, Q., Wang, Z., Weltje, G.J., Zhang, J., 2010. Dynamics and spatial variability of
506 near-bottom sediment exchange in the Yangtze Estuary, China. *Estuarine, Coastal and Shelf
507 Science* 86, 322-330.

508 Liu, W.Y., Tang, J.H., Miu, S.Q., 2011a. Study on evolution trend of North Channel of
509 Yangtze River Estuary and influences of related projects. *Yangtze River* 42, 39-43 (in
510 Chinese).

511 Liu, G.F., Zhu, J.R., Wang, Y.Y., Wu, H., Wu, J.X., 2011b. Tripod measured residual currents
512 and sediment flux impacts on the silting of the Deepwater Navigation Channel in the
513 Changjiang Estuary. *Estuarine, Coastal and Shelf Science* 93, 192-201.

514 Mao, Z.C., Shen, H.T., Liu, J.T., Eisma, D., 2001. Types of saltwater intrusion of the Yangtze
515 Estuary. *Science in China (Series B)* 44, 150-157 (in Chinese).

516 Nichols, M.M., Howard-Strobel, M.M., 1991. Evolution of an urban estuarine harbor: Norfolk,
517 Virginia. *Journal of Coastal Research* 7, 745-757.

518 Omar, K., Ahmad, A.B., Jean-philippe, G., Mustapha, J., 2016. Impact of Demographic
519 Growth on Seawater Intrusion: Case of the Tripoli Aquifer, Lebanon. *Water* 8, 1-18.

520 Pu, X., Shi, J.Z., Hu, G.D., Xiong, L.B., 2015. Circulation and mixing along the North
521 Passage in the Changjiang River Estuary, China. *Journal of Marine Systems* 148, 213-235.

522 Savenije HHG, 2005. *Salinity and tides in alluvial estuaries*. Elsevier, Amsterdam, p194.

523 Song, D.H., Wang, X.H., Cao, Z.Y., Guan, W.B., 2013. Suspended sediment transport in the
524 Deepwater Navigation Channel, Yangtze River Estuary, China, in the dry season 2009: 1.
525 Observations over spring and neap tidal cycles. *Journal of Geophysical Research – Oceans*
526 118, 5555-5567.

527 Song, D.H., Wang, X.H., 2013. Suspended sediment transport in the Deepwater Navigation
528 Channel, Yangtze River Estuary, China, in the dry season 2009: 2. Numerical simulations.
529 *Journal of Geophysical Research: Oceans* 118, 5568-5590.

530 Thomas, C.G., Spearman, J.R., Turnbull, M.J., 2002. Historical morphological change in the
531 Mersey estuary. *Continental Shelf Research* 22, 1775-1794.

532 Talke, S.A., de Swart, H.E., Schuttelaars, H.M., 2009. Feedback between residual circulations
533 and sediment distribution in highly turbid estuaries: an analytical model. *Continental Shelf*
534 *Research* 29, 119-135.

535 Van der Wal, D., Pye, K., Neal, A., 2002. Long-term morphological change in the Ribble
536 Estuary, northwest England. *Marine Geology* 189, 249–266.

537 Van der Wal, D., Pye, K., 2003. The use of historical bathymetric charts in a GIS to assess
538 morphological change in estuaries. *The Geographical Journal* 169, 21–31.

539 Wu, H., Zhu, J.R., Chen, B.R., Chen, Y.Z., 2006. Quantitative relationship of runoff and tide
540 to saltwater spilling over from the North Branch in the Changiang estuary: a numerical study.
541 *Estuarine, Coastal and Shelf Science* 69, 125-132.

542 Wu, J.X., Wang, Y.H., Cheng, H.Q., 2009. Bedforms and bed material transport pathways in
543 the Changjiang (Yangtze) Estuary. *Geomorphology* 104, 175-184.

544 Wu, H., Zhu, J.R., 2010. Advection scheme with 3rd high-order spatial interpolation at the
545 middle temporal level and its application to saltwater intrusion in the Changjiang Estuary.
546 *Ocean modeling* 33, 33-51.

547 Yang, S.L., Zhang, J., Dai, S.B., Li, M., Xu, X.J., 2005. Effect of deposition and erosion
548 within the main river channel and large lakes on sediment delivery to the estuary of the
549 Yangtze River. *Journal of Geophysical Research* 112, F02005. doi:10.1029/2006JF000484.

550 Yang, Z.Y., Cheng, H.Q., Li, J.F., 2015a. Nonlinear advection, Coriolis force, and frictional
551 influence in the South Channel of the Yangtze Estuary, China. *Science China Earth Sciences*
552 58, 429-435 (in Chinese).

553 Yang, Y., Chen, X.F., Li, Y.Y., Xiong, M., Shen, Z.Y., 2015b. Modeling the effects of
554 extreme drought of pollutant transport processes in the Yangtze River Estuary. *Journal of the*
555 *American water resources association* 51, 625-636.

556 Yuan, R., Zhu, J.R., 2015. The Effects of Dredging on Tidal Range and Saltwater Intrusion in
557 the Pearl River Estuary. *Journal of Coastal Research* 31, 1357-1362.

558 Zhou, M.J., Shen, Z.L., Yu, R.C., 2008. Responses of a coastal phytoplankton community to
559 increased nutrient input from the Changjiang (Yangtze) River. *Continental Shelf Research* 28,
560 1483-1489.

561 Zhang, Q., Xu, C.Y., Singh, V.P., Yang, T., 2009. Multiscale variability of sediment load and
562 streamflow of the lower Yangtze River basin: Possible causes and implications. *Journal of*
563 *Hydrology* 368, 96–104.

564 Zhao, H., Zhou, J.L., Zhao, J., 2015. Tidal impact on the dynamic behavior of dissolved
565 pharmaceuticals in the Yangtze Estuary, China. *Science of the Total Environment* 536,
566 946-954.

567 Zhu, W.W., Li, J.F., Sanford, L.P., 2015. Behavior of suspended sediment in the Changjiang
568 Estuary in response to reduction in river sediment supply. *Estuaries and Coasts* 38,
569 2185-2197.

Table 1. Bathymetric charts used as the main source for morphological change analysis for the Yangtze River Estuary.

Year	Channel	Scale	Source
2002	South and North Channels, South and North Passages and Hengsha Passage	1:10000	CJWAB
2007	North Channel and Hengsha Passage	1:10000	CJWAB
2010	South and North Passages	1:60000	SECSRC
2013	South Channel, South and North Passages	1:60000	SECSRC
	North Channel and Hengsha Passage	1:15000	Maritime safety administration of P.R.C.

CJWAB: Changjian Estuary Waterway Administration Bureau (CJWAB), Ministry of Transportation of China.

SECSRC: Shanghai Estuarine & Coastal Science Research Center.

Table 2. Changes of six cross-sectional areas in the North Channel and South Channel (negative means increase, plus means decrease)

	NC1	NC2	NC3	SC1	SC2	SC3
	m ²	m ²	m ²	m ²	m ²	m ²
2002	54973	45620	36392	59726	58293	55409
2007	56343	44905	40372			
2013	61811	45514	36280	65537	65482	61955
2002-2013	12.4%	-0.2%	-0.3%	9.7%	12.3%	11.8%

Table 3. Changes of eight cross-sectional areas in the Hengsha Passage and the South Passage (negative means increase, plus means decrease)

	HP1	HP2	HP3	SP1	SP2	SP3	SP4	SP5
	m ²	m ²	m ²	m ²	m ²	m ²	m ²	m ²
2002	9122	8255	9109	29327	25265	39521	92169	92453
2007	13126	7062	8906					
2010				33175	29402	43034	85563	100380
2013	21634	12086	13668	34631	29981	44513	85405	100424
2002-2013	137.2%	46.4%	50%	18.1%	18.7%	12.6%	-7.3%	8.6%

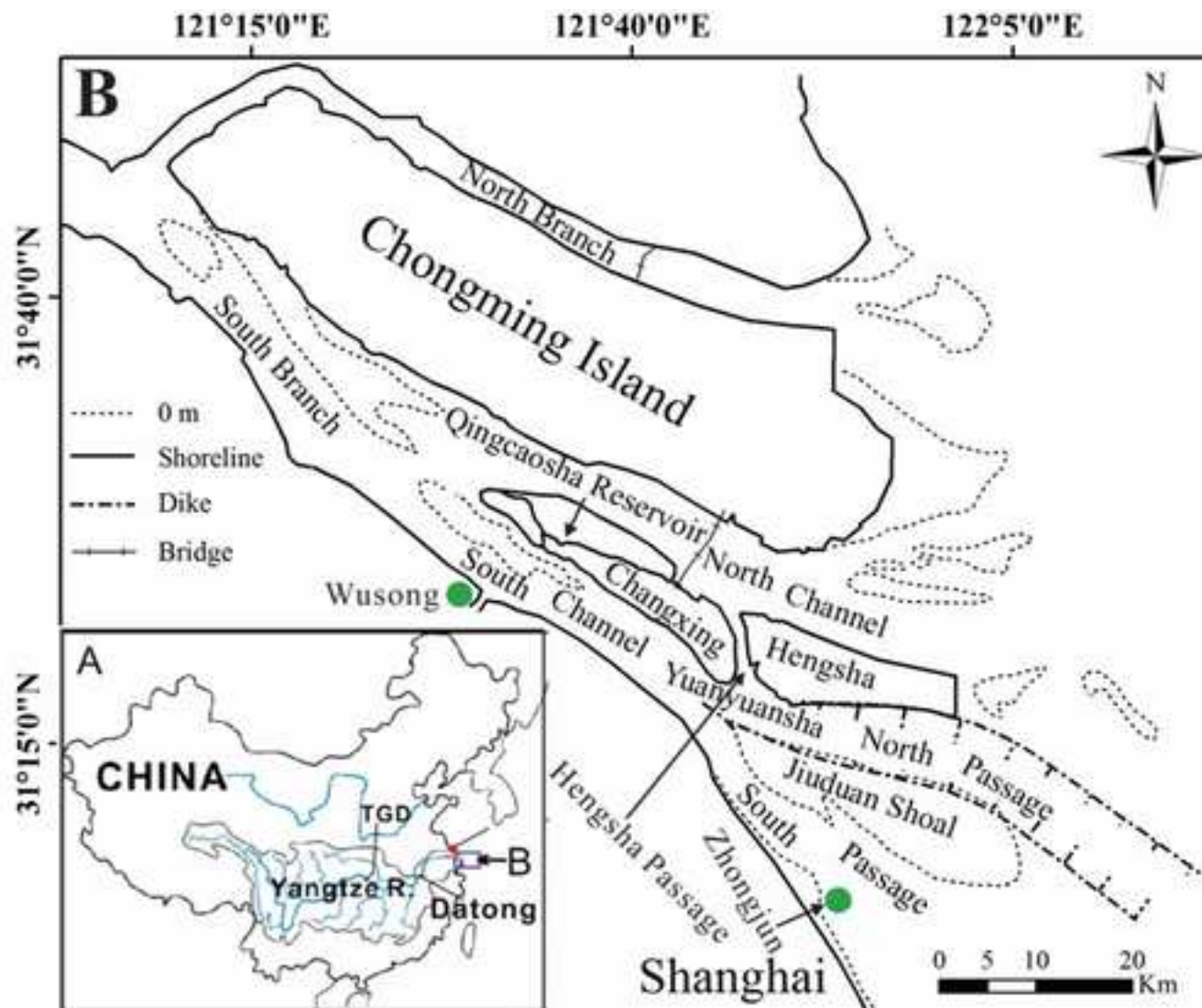


Fig. 1. Geographical location of the study area – the Yangtze River Estuary in China, with Chongming Island, the Changxing Island, Hengsha Island, the North and South Branches, the North and South Channels Passages, Hengsha Passage and the Jiuquan Shoal.

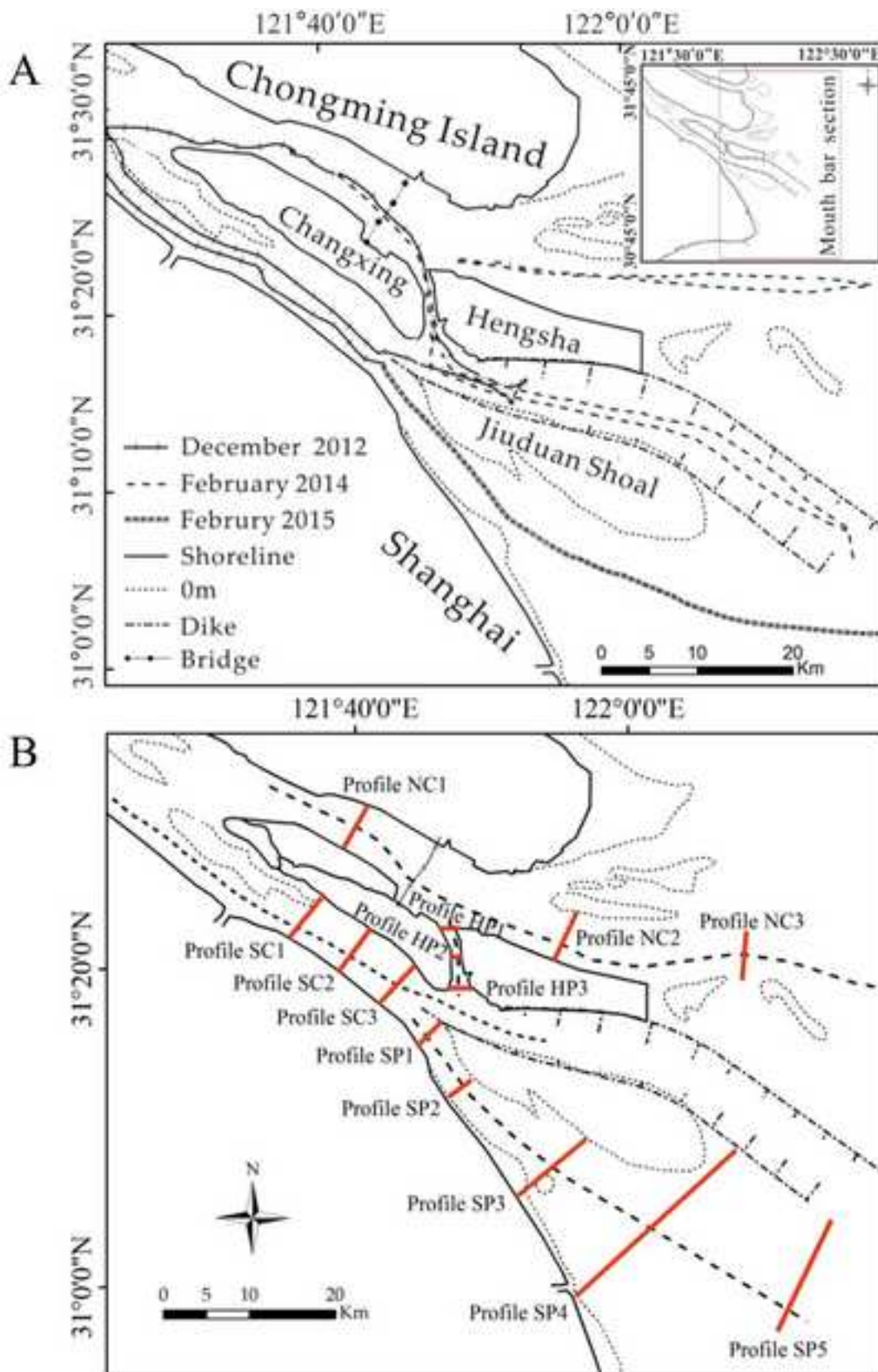


Fig. 2. Field measurement routes and location of the mouth bar section of the Yangtze River Estuary (A). Location of 14 cross sections (red solid lines) and 4 longitudinal sections (black dotted lines) along the North Channel and South Channels, the Hengsha Passage and the South Passage (B).

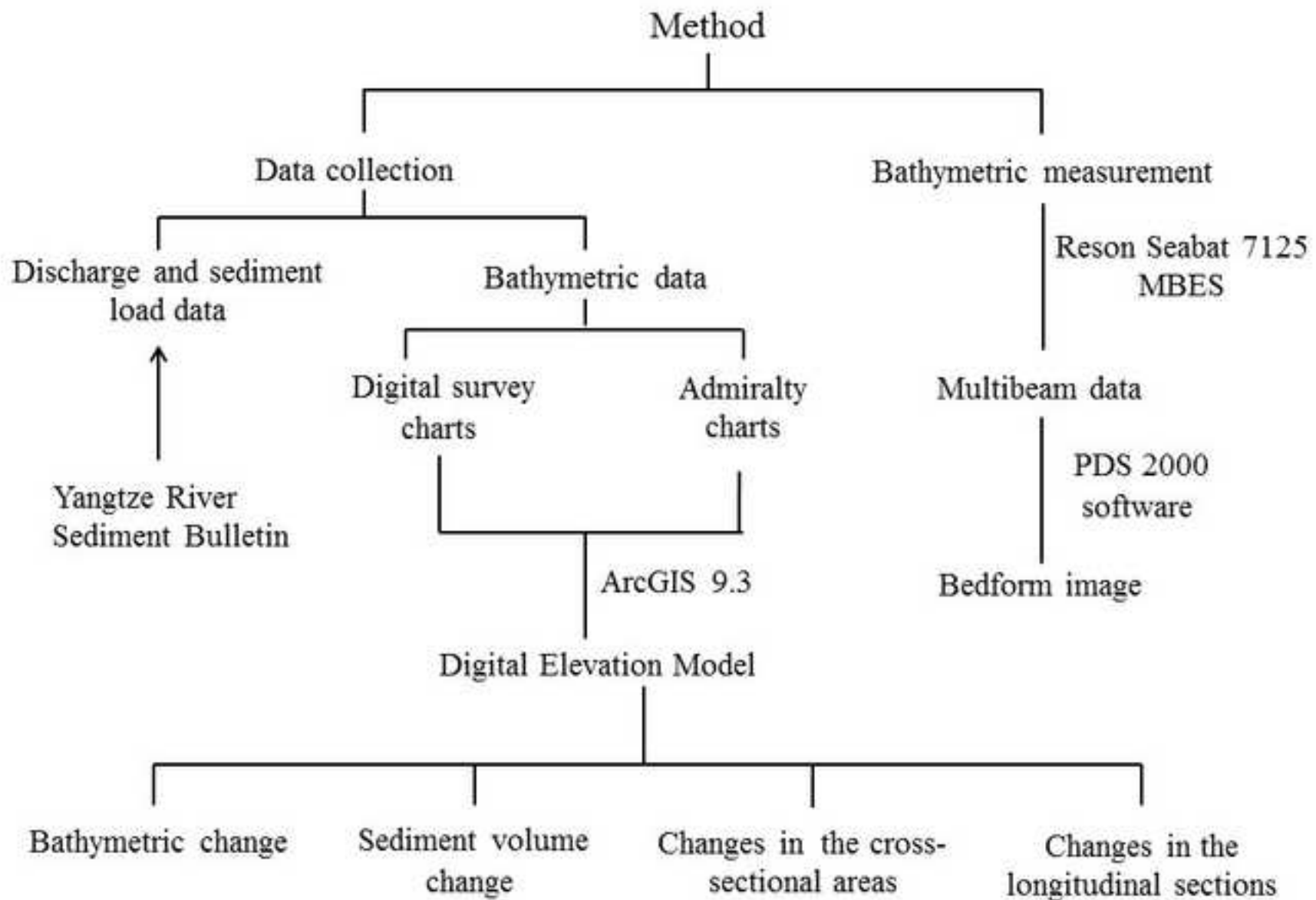


Fig. 3. Schematic diagram of the data collection and analysis in the present study

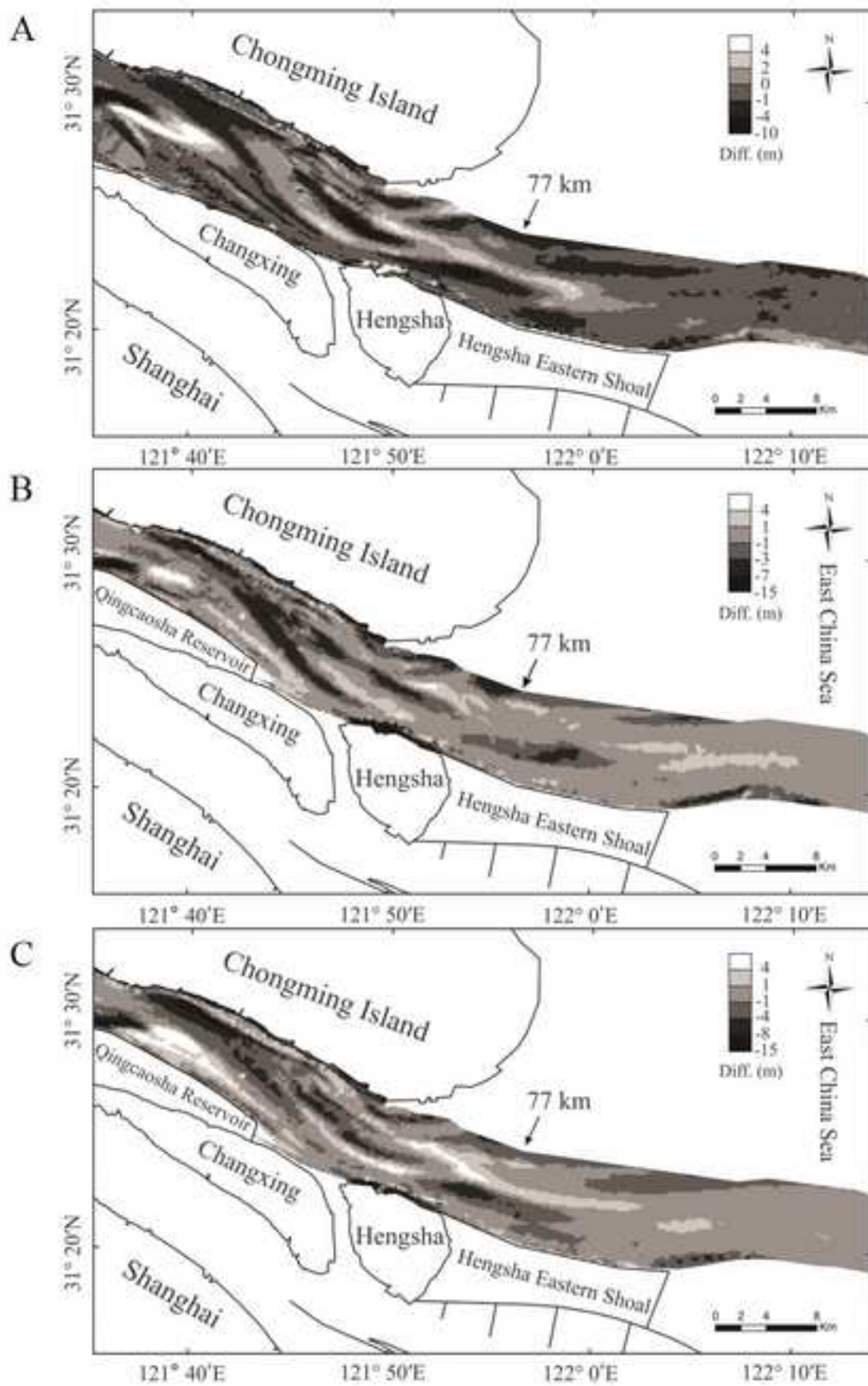


Fig. 4. Bathymetric elevation changes in the North Channel from 2002 to 2007 (A), 2007 to 2013 (B) and 2002 to 2013 (C) (negative values indicate net erosion; positive values indicate net accretion).

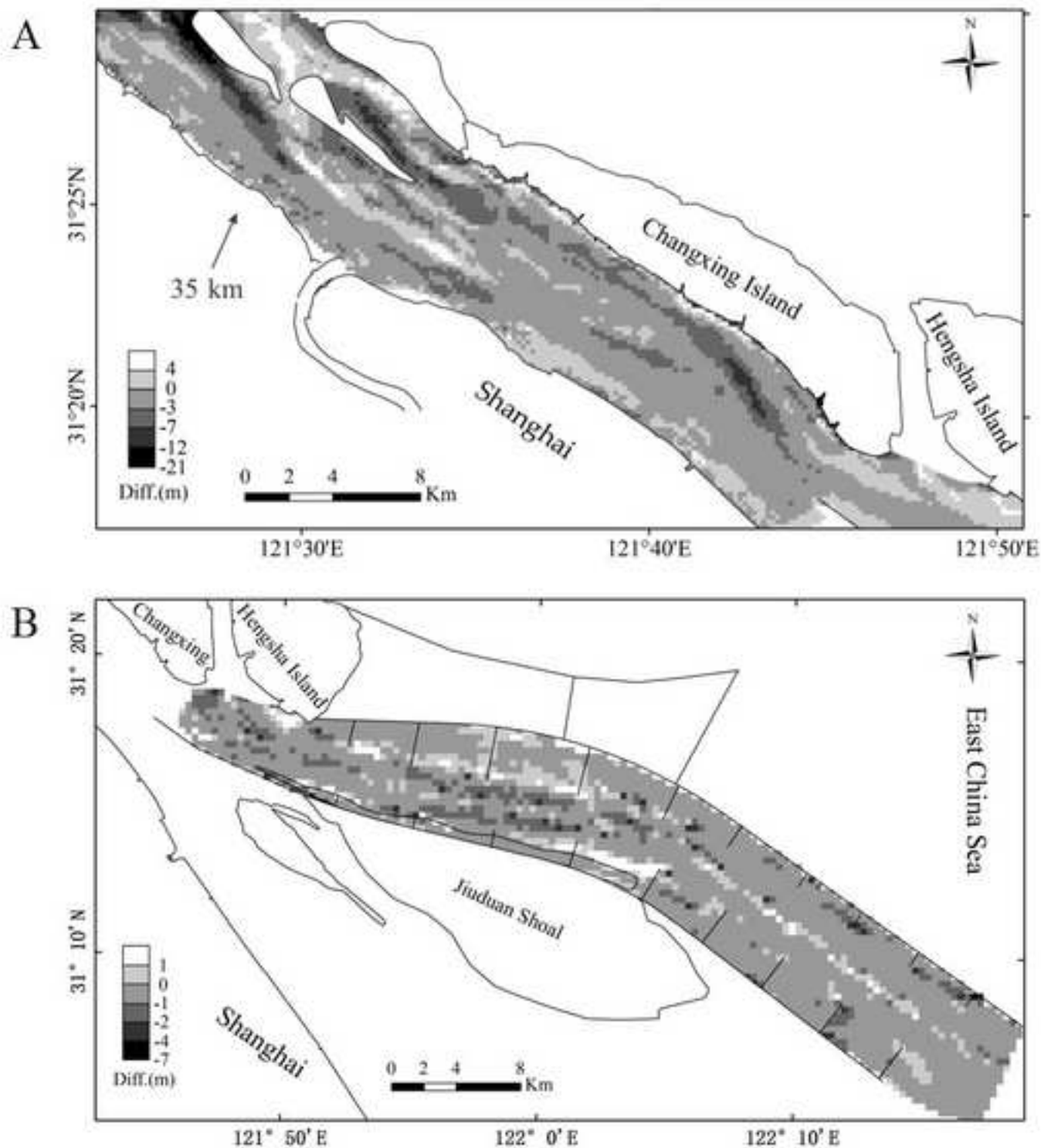


Fig. 5. Bathymetric elevation changes in the South Channel from 2002 to 2013 and in the North Passage from 2010 to 2013 (negative means erosion, positive means deposition).

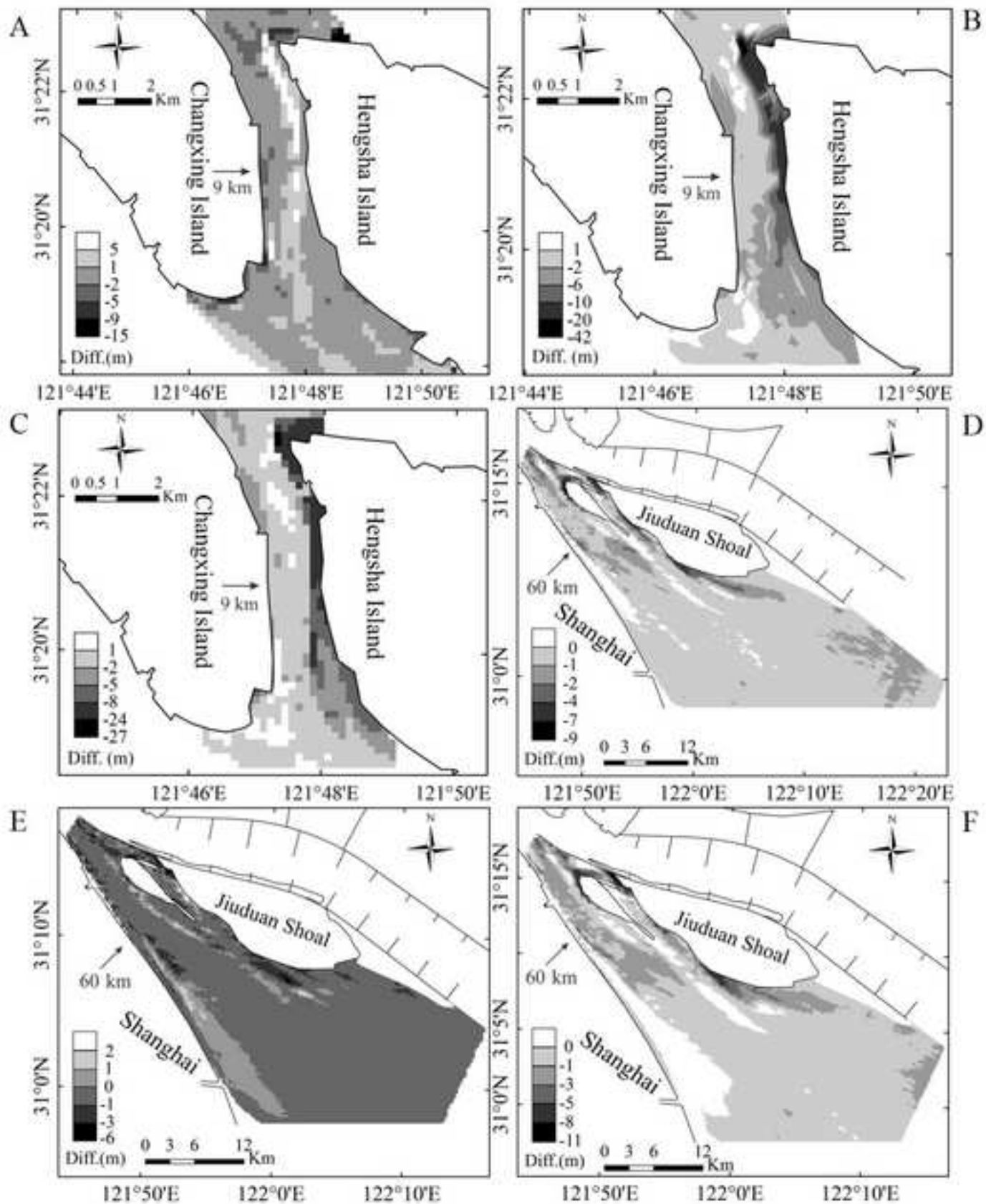


Fig. 6. Bathymetric elevation changes in the Hengsha Passage from 2002 to 2007 (A), 2007 to 2013 (B) and 2002 to 2013 (C), and in the South Passage from 2002 to 2010 (D), 2010 to 2013 (E) and 2002 to 2013 (F) (negative means erosion, positive means deposition).

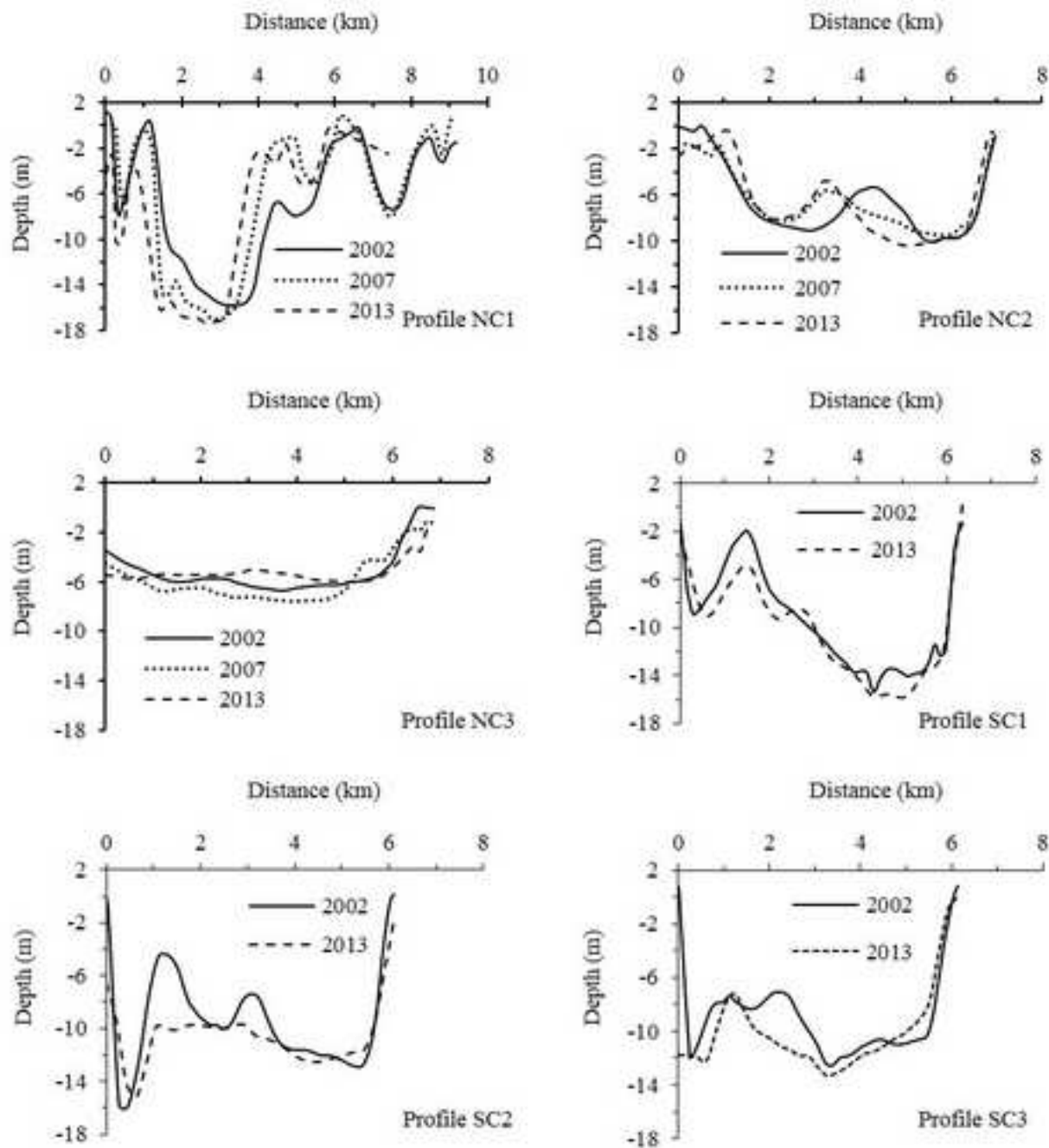


Fig. 7. Channel profiles at 6 different cross-sections (for location see Fig. 2B) in 3 or 2 different years in the North and South Channels. Distance was measured with respect to the northern edge of these cross-sections.

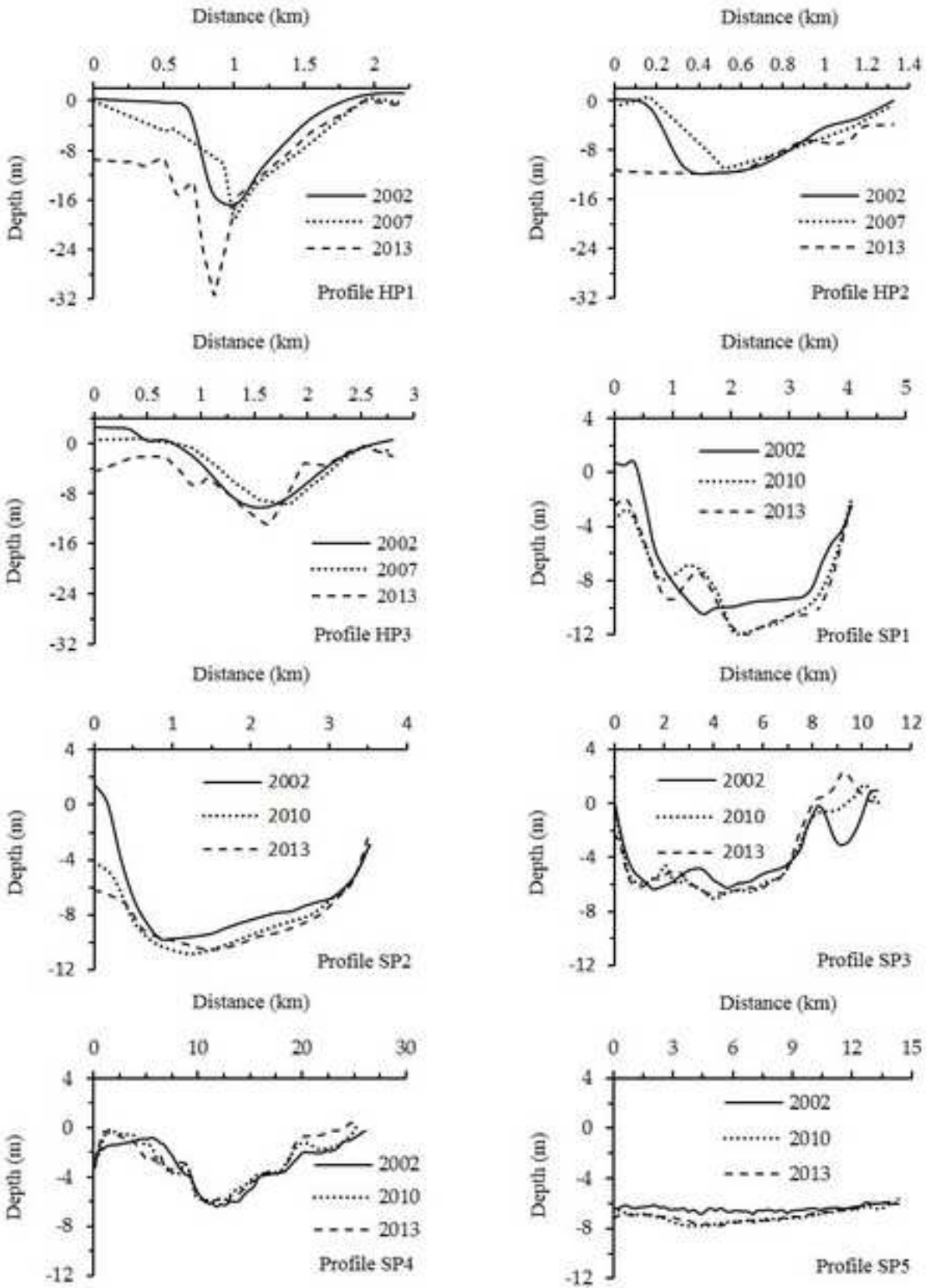


Fig. 8. Channel profiles at 8 different cross-sections (for location see Fig. 2B) in 3 different years in the Hengsha Passage and the South Passage. For the Hengsha Passage and the South Passage, distance was measured with respect to the eastern edge and northern edge of the cross-sections, respectively.

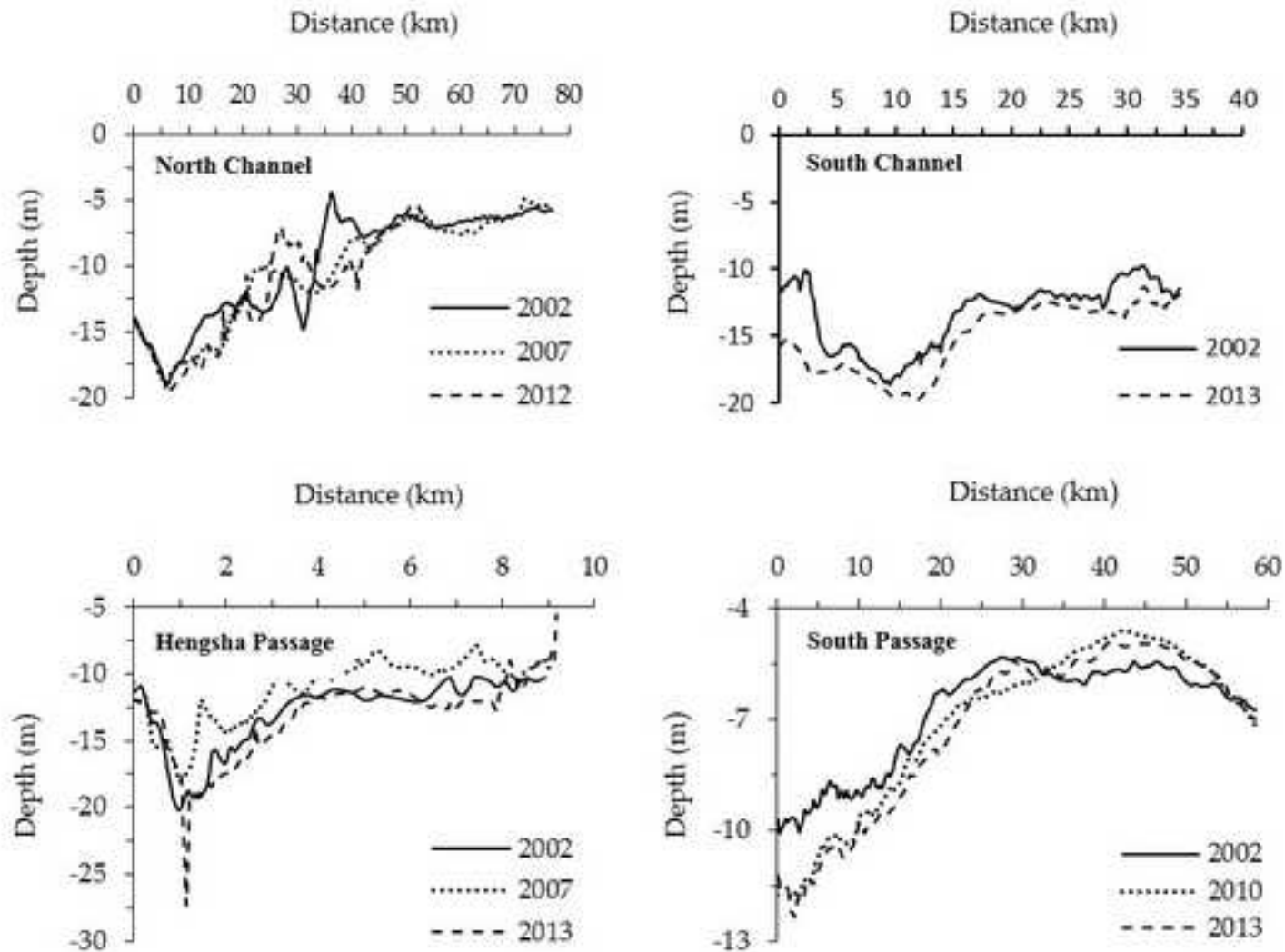


Fig. 9. Longitudinal changes of thalweg of the four studied channels in the lowermost Yangtze River Estuary (for locations see Fig. 2B) in 3 or 2 different years. Distance was measured with respect to the western edge of the profiles in the South and North Channels and the South Passage. For the Hengsha Passage, distance was measured with respect to the northern edge of the profile.

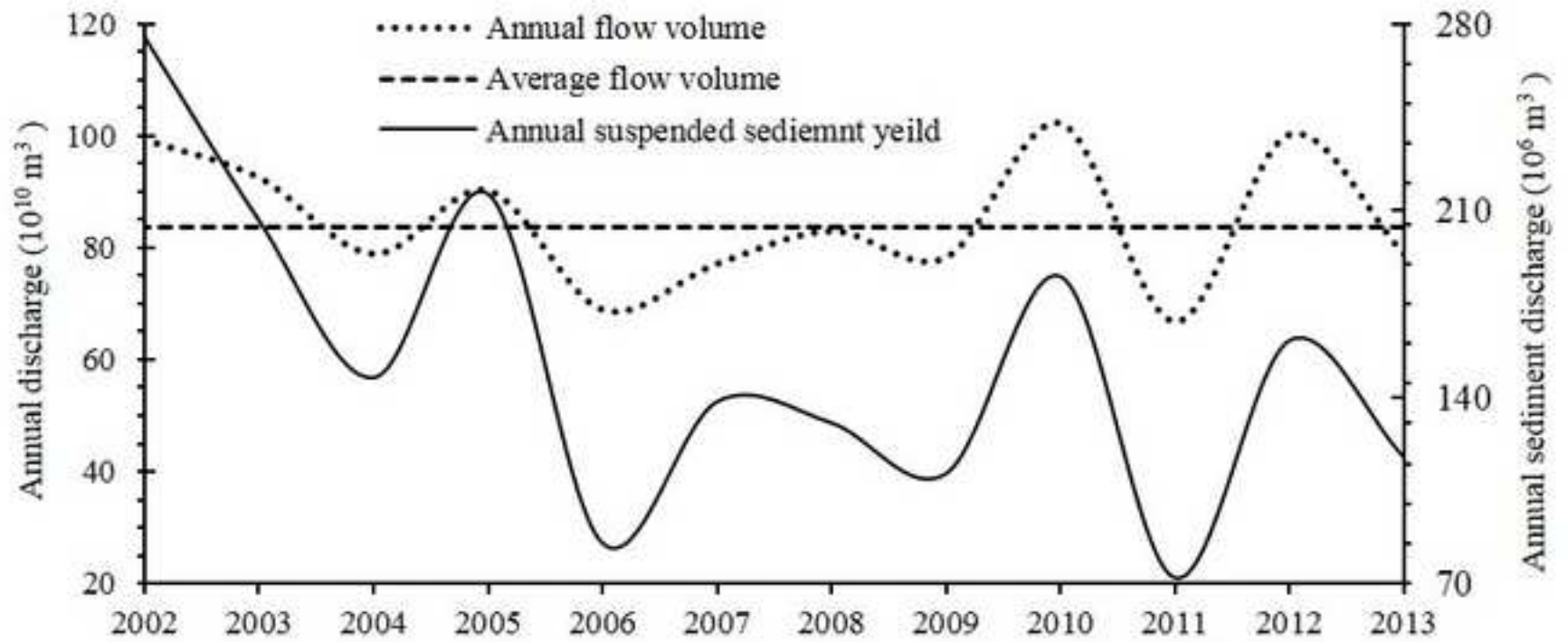


Fig. 10. Trend of the annual flow volume and suspended sediment yield at the Datong station on the Yangtze River in the past decade.

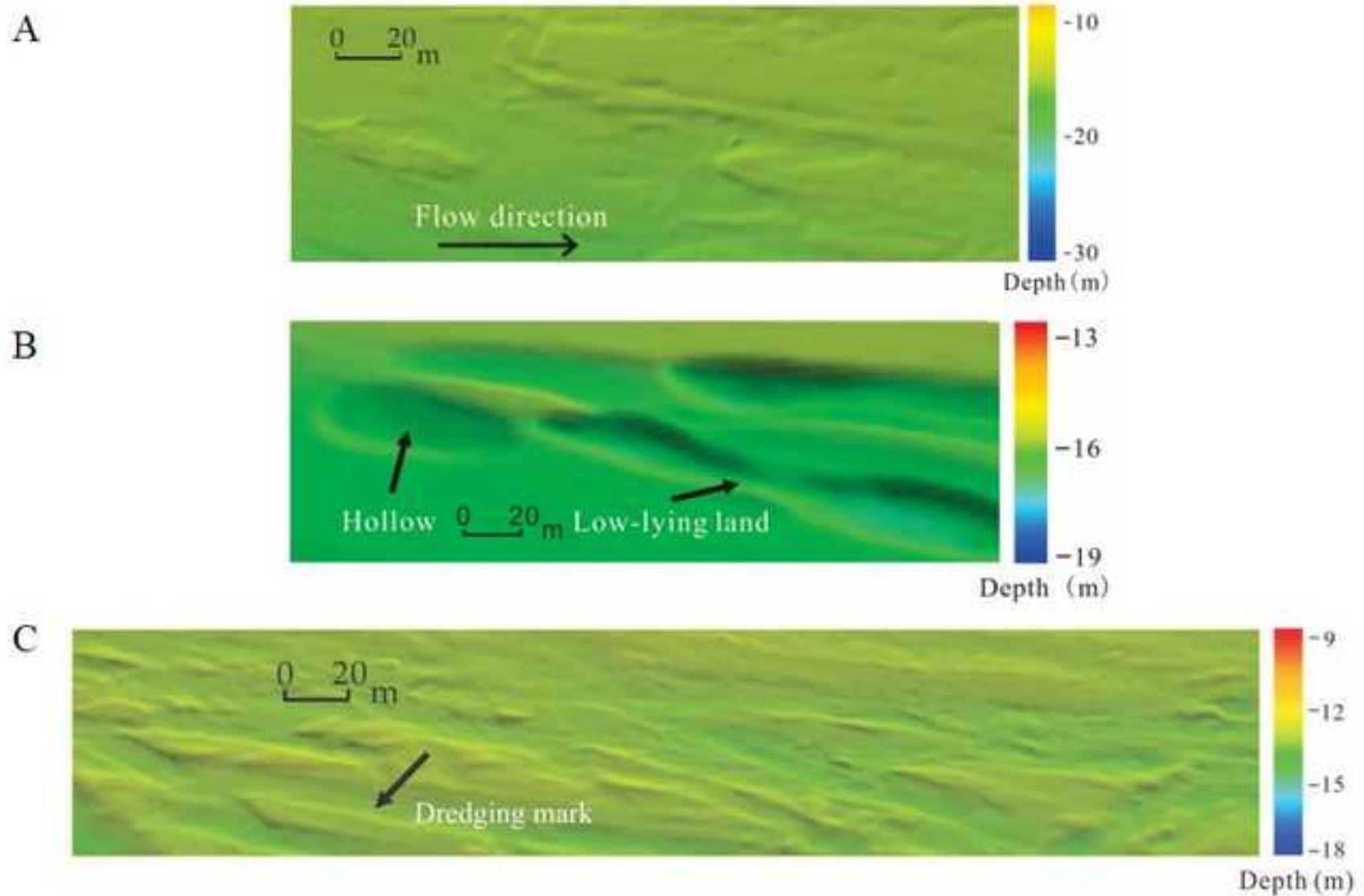


Fig. 11. Scour mark (A) in the Hengsha Passage, and hollow (B) and dredging mark (C) in the North Passage (measured in February 2014).